Desalination and Water Treatment
www.deswater.com
doi: 10.1080/19443994.2013.793915

51 (2013) 6507–6516
October

Taylor & Francis
Taylor & Francis Group

Adsorption of acid red18 dye from aqueous solution using single-wall carbon nanotubes: kinetic and equilibrium

Mohammad Shirmardi[a], Amir Hossein Mahvi[b,c,d,*], Alireza Mesdaghinia[b] Simin Nasseri[b], Ramin Nabizadeh[b]

[a]*Department of Environmental Engineering, School of Public Health, Ahvaz Jundishapur University of Medical Sciences, Ahvaz, Iran*
[b]*Department of Environmental Engineering, School of Public Health, Tehran University of Medical Sciences, Tehran, Iran*
email: ahmahvi@yahoo.com
[c]*Center for Solid Waste Research, Institute for Environmental Research, Tehran University of Medical Sciences, Tehran, Iran*
[d]*National Institute of Health Research, Tehran University of Medical Sciences, Tehran, Iran*

Received 29 October 2011; Accepted 14 March 2013

ABSTRACT

Dyes or colors are one of the most important chemicals used in textile industries. It is necessary that dye-contaminated wastewater before discharging to environment treated by an appropriate and effective method. In this study, the performance of single-wall carbon nanotubes (SWCNTs) as an adsorbent for the removal of dye from aqueous solution was evaluated. The effect of operational parameters, such as contact time, solution pH, adsorbent dosage, and initial dye concentration was studied. Adsorption data were analyzed using Langmuir, Freundlich, and Temkin adsorption isotherms. The Langmuir isotherm ($R^2 = 0.9844$) was the best fitted graph for experimental data with maximum adsorption capacity (q_m) of 166.667 mg/g. The kinetic data were tested using pseudo-first-order, pseudo-second-order, and intraparticle diffusion models. The results of this study indicate that SWCNTs can be used as an effective adsorbent for the removal of azo dyes.

Keywords: Carbon nanotubes; Adsorption; Azo dye; Kinetics; Equilibrium; Isotherm

1. Introduction

Synthetic dyes are widely used in various industries, such as textiles, paper, leather, printing, and cosmetics. Discharging wastewater containing dyes causes the serious environmental problems because of its high toxicity, possible accumulation in the environment, and the complex aromatic structure make them more stable and more difficult to remove from effluent discharged to the hydrosphere [1,2]. Therefore, industrial effluents containing dyes need to be treated before discharging to the environment [3]. Additionally, most of these dyes can cause allergy, dermatitis, skin irritation, and also provoke cancer and mutation in humans [4,5]. There are several methods for dye removal, such as aerobic and anaerobic digestion, coagulation, advanced oxidation, combined chemical and biochemical process, adsorption, and membrane treatment; each of these has different removal efficiency, advantage,

*Corresponding author.

disadvantage, capital costs, and operating rates. The adsorption technique has proven to be an effective and attractive process for wastewater treatment in terms of initial cost, simplicity of design, ease of operation, and insensitivity to toxic substances. In addition, this technique can produce high-quality effluent that does not result in the formation of harmful substances, such as ozone and free radicals [6–9]. Numerous adsorbents such as activated carbon [10], bagasse fly ash [11], babassu coconut epicarp [12], and chitosan nanodispersion [13] have been examined for their ability to remove dyes from wastewater. Among these materials activated carbon is widely used adsorbent for environmental pollution control. More recently, Long and Yang [14] reported that multi-wall carbon nanotubes (MWCNTs) could be more efficient for the removal of dioxin than activated carbon; carbon nanotubes (CNTs) as new adsorbents have gained increasing attention of many researchers. According to the layers involved, CNTs can be classified into single-wall carbon nanotubes (SWCNTs) and MWCNTs. Because of their relatively large specific surface areas, small size, unique hollow structures, high mechanical strength, and remarkable electrical conductivities, CNTs have been proven to possess great potential as superior adsorbents for removing many kinds of organic and inorganic contaminants [15,16], such as heavy metal, trihalomethanes, fluoride, and dyes from water and wastewater [17–21]. Since removal of dyes by SWCNTs have been less investigated, the present work focuses on the removal of anionic dye (Acid Red 18, AR18) by SWCNTs from aqueous solution. The influence of different variable, including contact time, pH of solution, adsorbent dosage, and initial dye concentration was evaluated. Adsorption isotherms and kinetics were also analyzed.

2. Materials and methods

2.1. Materials

The CNTs used in this study were SWCNTs. These CNTs have specific surface area 700 m^2/g and electrical conductivity 3,000 S/m. The inner diameter, the outer diameter, and the length of the SWCNTs are in the ranges of 0.8–1.1 nm, 1–2 nm and 10 μm, respectively. The purity of CNTs was more than 95%. The CNTs have been synthesized in the Iranian Research Institute of Petroleum Industry which were purchased and used without pretreatment for this study. Dyes containing (–N=N–) bands are known as azo dye. Since AR18 has an azo band, selected for this study, was purchased from Alvan Sabet Co (Hamedan, Iran), and was used without further purification. AR18 formula, molecular weight, and maximum adsorption wavelength (λ_{Max}), are $C_{20}H_{11}N_2Na_3O_{10}S_3$, 604.47 g/mol, and 506 nm, respectively. Chemical structure of dye is shown in Fig. 1. Stock solution of dye was prepared by weighting and dissolving the required amounts of AR18 in distiled water. Dye solutions with different initial concentrations were fabricated by diluting stock solution in required proportions and their absorbance were read by UV–Vis spectroscopy. After taking the measurements, calibration curve was made to obtain the concentration of each experiment. This curve was used to change the adsorption data into concentrations for kinetic and equilibrium studies. All other chemicals were of analytical grade.

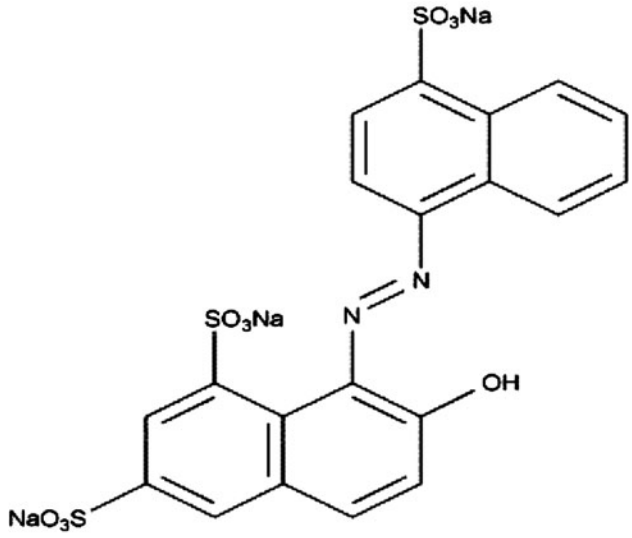

Fig. 1. Chemical structure of AR 18 dye.

2.2. Adsorption experiments

Batch adsorption experiments were conducted using 250 mL Erlenmeyer flasks containing 100 mL of dye solutions which were agitated at 175 rpm on an Illuminated Refrigerated Incubator Shaker (Innova 4340, USA). Initial solution pH was adjusted using 0.1 N HCl and 0.1 N NaOH. In this study, various parameters, such as contact time, solution pH, adsorbent dosage, and initial dye concentration were investigated. The effect of contact time evaluated by 0.02 g of SWCNTs was added to 100 mL of dye solution with different initial dye concentrations. At specific time intervals, samples were taken from the suspension and were analyzed. In these experiments different ranges of the solution pH were investigated to determine the effect of solution pH on the adsorption process. To determine the effect of adsorbent dose, different amounts of adsorbent were added into the different initial concentrations of AR18 solution, at

pH 3.0 at equilibrium time. In order to study the effect of AR18 initial concentration on the adsorption process, 100 mL of AR18 solutions with different initial concentrations was prepared in a series of 250 mL Erlenmeyer flasks and different adsorbent doses were added to each flask at pH 3.0. At the end of equilibrium time, in order to separate the adsorbents from the aqueous solutions, the samples were centrifuged at 4,000 rpm for 10 min, and then the supernatant of suspension was filtered using a 0.2 μm Millipore filter. The residual dye concentrations (AR18) were analyzed by UV–Visible spectrophotometer (Perkin-Elmer Lambda 25, USA) at maximum adsorption wavelength of 506 nm. The procedures of kinetic experiments were identical with those of equilibrium tests. The dye removal percentage, the amount of AR18 adsorbed at time t (q_t, mg/g) and at equilibrium (q_e, mg/g) was calculated through the following equations, respectively:

$$\text{Dye removal } \% = \frac{(C_o - C_e)}{C_o} \times 100 \quad (1)$$

$$q_e = \frac{(C_o - C_e) \times V}{M} \quad (2)$$

$$q_t = \frac{(C_o - C_t) \times V}{M} \quad (3)$$

where C_o and C_e (mg/L) are the initial and equilibrium concentrations of AR18, respectively. M (g) is the weight of SWCNTs and V (L) the volume of the solution, C_t is the concentration of dye at any time t, q_t (mg/g) is the amount of adsorbed dye on SWCNTs at any time.

3. Results and discussion

3.1. Effect of contact time

The effect of contact time on adsorption of AR18 by SWCNTs at different initial dye concentrations (25, 50, 75, and 100 mg/L) is presented in Fig. 2. As shown in Fig. 2, by increasing the contact time the amount of adsorbed dye on SWCNTs at any time was increased. The results show that the adsorption of AR18 is faster during initial stages, then becomes slow and finally reaches to equilibrium at approximately 100 min. It was observed that removal efficiency of dye increased with the increase in contact time for all initial AR18 concentrations. These observation show that initial dye concentration has no effect on required time for equilibrium. The fast adsorption rate during initial stages is probably due to the availability of a large number of vacant sites on the surface of adsorbent and with the gradual occupancy of these sites, the adsorption became less efficient. With increasing time due to the increased repulsive forces between dye molecules and bulk solution, occupation of the remaining vacant sites is more difficult [22,23].

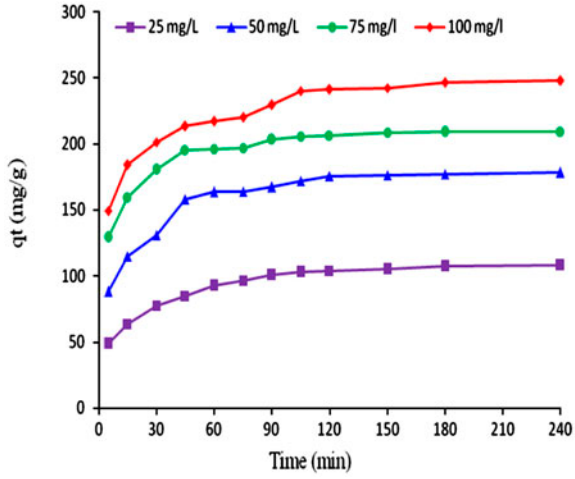

Fig. 2. Effect of contact time on the removal of AR18 dye by SWCNTs at different dye concentration (condition: adsorbent dose = .02 g, T = 25°C, pH = 7).

3.2. Effect of solution pH

Solution pH is one of the most important parameters that affect adsorption of dye molecules. The effect of solution pH on removal of AR18 on SWCNTs was studied at different pH values at different dye concentrations while the adsorbent dosage, contact time, and temperature were fixed at 0.04 g, 100 min, and 25°C, respectively. The effect of solution pH on removal of AR18 is presented in Fig. 3. As shown in Fig. 3, dye removal efficiency decreased when the pH increased from 3 to 9 for all dye concentrations, indicating that pH significantly affected AR18 removal percentage, particularly under acidic conditions. For initial dye concentration 25 mg/L removal of AR18 decreased from 98 to 74% when the pH increased from 3 to 9. Therefore, the pH 3 is selected as optimum pH for the other experiments. The dissolved AR18 dye is negatively charged in water solution, and then the removal of this dye takes place when the adsorbents present a positive surface charge. Acidic condition increases the electrostatic attraction between anionic dye and partially positive charged SWCNTs surface. With the increase of the pH value (basic condition) the number

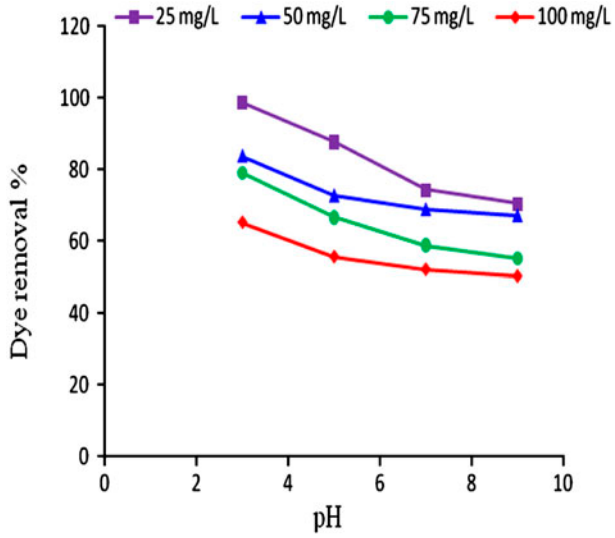

Fig. 3. Effect of initial pH on the removal of AR18 by SWCNTs at different dye concentration (condition: adsorbent dose = .04 g, $T = 25°C$).

of positively charged sites decreases and the number of negatively charged sites increases [24,25].

3.3. Effect of adsorbent dosage

The effect of adsorbent dose on removal of AR18 for different initial dye concentration 25, 50, 75, and 100 mg/L were investigated. Fig. 4 shows the removal of AR18 as a function of SWCNTs dosage. As shown in Fig. 4, for initial dye concentration 25 mg/L the removal percentage increased from 89 to 98% when SWCNTs increased from 0.02 to 0.06 g. The increase in percentage of dye removed with an adsorbent dosage that can be attributed to the availability of more surface area of the SWCNTs [3]. Similar observations can be found in previous literature. Ehrampoush et al. [26] who utilize eggshell for the removal of reactive red 123 suggested that increasing of ES dose in aqueous solution can result to increased pollutant removal, but this elevation of ES leads to decreasing of adsorbed dye per unit of adsorbent (q_e). Similar results were also obtained for Brazilian pine-fruit shell as a biosorbent by Eder C. Lima et al. [27] and for activated carbon prepared from agricultural waste by Senthilkumaar et al. [28].

3.4. Effect of initial dye concentration

The dye concentration is another important variable that can affect dye removal process. Fig. 5 shows the effect of initial AR18 concentration on removal of dye by SWCNTs. From the figure, it is evident that by increasing the initial dye concentration the percentage removal of dye decreased, although the actual amount of dye adsorbed per unit mass of SWCNTs increased with the increase in initial concentration. As the initial dye concentrations increase from 25 to 100 mg/L, the percentage removal of dye decreases from 98 to 82% at 0.06 g adsorbent dosage. However, the amount of AR18 adsorbed at equilibrium increased from 41 to 136 mg/g. This is due to the increase in the driving force of the concentration

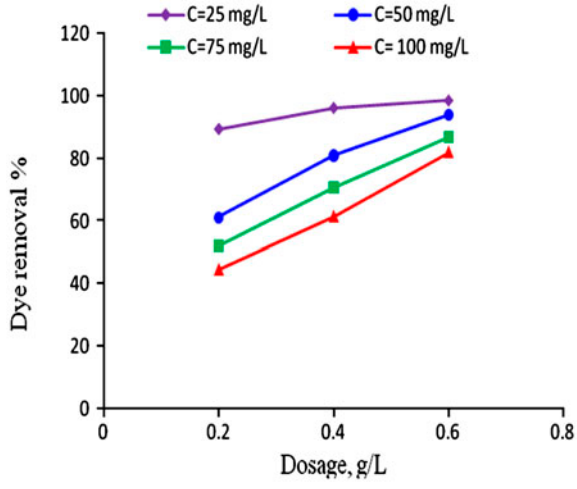

Fig. 4. Effect of adsorbent dosage on the removal of AR18 by SWCNTs at different dye concentration (condition: $T = 25°C$, pH = 3).

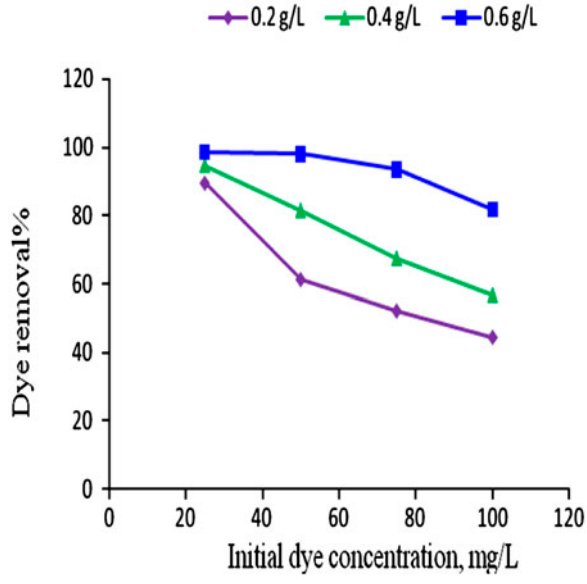

Fig. 5. Effect of initial dye concentration on the removal of AR18 by SWCNTs at different adsorbent dosage (condition: adsorbent dose = .04 g, $T = 25°C$, pH = 3).

gradient with the higher initial dye concentrations [29]. Similar results have been reported in literature [22,24].

3.5. Adsorption isotherms

The adsorption isotherm is the most important information, which indicates how the adsorbate interacts with adsorbents, and is basically important to describe how the adsorption molecules distribute between the liquid phase and the solid phase when the adsorption process reaches equilibrium, give valuable information to optimize the design of an adsorption system [30,31]. Three important isotherms, the Langmuir, Freundlich, and Temkin isotherms were used to fit the experimental data for AR18 adsorption equilibrium in aqueous solution on SWCNTs at different initial dye concentration.

3.5.1. Langmuir isotherm

The Langmuir adsorption isotherm has been the most widely used adsorption isotherm for the adsorption of a solute from a liquid solution, which is based on the assumption of monolayer adsorption on a structurally homogeneous adsorbent, where all the sorption sites are identical and energetically equivalent [32]. The saturation monolayer can be represented by the expression:

$$q_e = \frac{q_m K C_e}{1 + K C_e} \tag{4}$$

The linear form of Langmuir equation is:

$$\frac{C_e}{q_e} = \frac{1}{K q_m} + \frac{C_e}{q_m} \tag{5}$$

where q_e is the amount of dye adsorbed per gram of SWCNTs (mg/g); C_e is the equilibrium concentration of dye in a solution (mg/L); K is the Langmuir constant (L/mg), which is related to the affinity of binding sites; and q_m is the theoretical saturation capacity of the monolayer (mg/g). The values of K and q_m were calculated from the linearized form of Eq. (5) by plotting C_e/q_e vs. C_e.

3.5.2. Freundlich isotherm

The Freundlich isotherm is an empirical equation and corresponds to the heterogeneous adsorbent surfaces. Freundlich equation is expressed as [17,33]:

$$q_e = k_f C^{1/n} \tag{6}$$

The linear form of Freundlich equation is:

$$\log q_e = \log(k_f) + 1/n \log(C_e) \tag{7}$$

where q_e is the amount of AR18 adsorbed per unit mass of adsorbent (mg/g), C_e is the concentration of AR18 in solution at equilibrium (mg/L), k_f and n are the Freundlich constants, which correspond to the adsorption capacity and the adsorption intensity of the adsorbent, respectively, which can be calculated from the logarithmic plot of q_e vs. C_e.

3.5.3. Temkin equation

Temkin isotherm [2,32,34] contains a factor that explicitly takes into account the adsorptive–adsorbent interactions, Temkin equation is:

$$q_e = B_1 \ln(k_t C_e) \tag{8}$$

The linear form of Temkin isotherm is expressed as:

$$q_e = B_1 \ln k_t + B_1 \ln C_e \tag{9}$$

where $B_1 = RT/b$ and k_t are the constants. R is the gas constant (8.31 J/mol K) and T (K) is the absolute temperature, k_t is the equilibrium binding constant (L/mg) corresponding to the maximum binding energy and constant B_1 is related to the heat of adsorption. The isotherm constants k_t and B_1 can be obtained from the slope and intercept of plots (q_e vs. ln C_e), respectively. The isotherm constants for all above-mentioned isotherms were calculated from the linear form of each model for different initial dye concentration. The parameters for the three isotherm models and the cor-

Table 1
The parameters of Langmuir, Freundlich, and Temkin isotherm models

Isotherm models	Parameters	Value
Langmuir	q_m (mg/g)	166.667
	k (L/mg)	0.335
	R^2	0.985
Freundlich	k_f (mg/g (L/mg)1/n)	54.41
	n	3.51
	R^2	0.951
Temkin	B	21.703
	k_t	3.135
	R^2	0.983

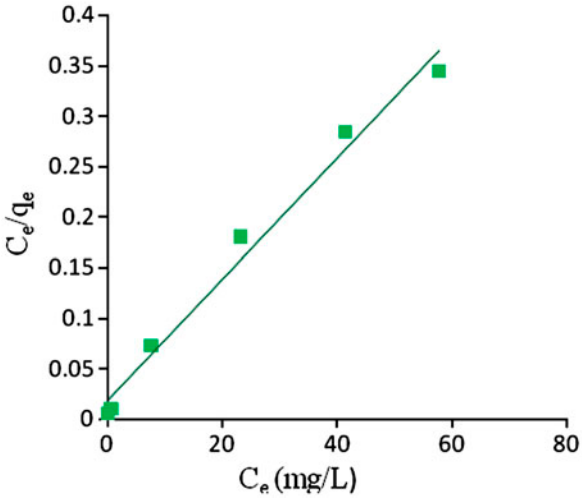

Fig. 6. Langmuir isotherm plot for removal of AR18 by SWCNTs (condition: initial dye concentration = 10, 25, 50, 75, 100, and 120 mg/L, adsorbent dose = .04 g, $T = 25°C$, pH = 7).

relation coefficients are given in Table 1. Fig. 6 (a, b, c) present the Langmuir, Freundlich, and Temkin isotherms of AR18, respectively. Based on the correlation coefficient (R^2) (Table 1), it can be seen that the adsorption of AR18 onto SWCNTs is best fitted in the Langmuir isotherm than the other two isotherms. The maximum adsorption capacity obtained from the Langmuir isotherm is 166.666 mg/g. Comparative values of maximum adsorption capacity for some of the adsorbents for different dyes removal, are given in Table 2.

3.6. Adsorption kinetics study

Various models are available to express the mechanism of solute sorption onto a sorbent. In this study, the experimental equilibrium data of AR18 onto SWCNTs were analyzed by pseudo-first-order kinetic model, pseudo-second-order kinetic model, and intraparticle diffusion. These models are widely used for describing dyes sorption as well as other pollutants such as heavy metals on solid adsorbents. The best-fit model was chosen based on the linear regression correlation coefficient values, R^2.

3.6.1. Pseudo-first-order model

Pseudo-first-order model can be expressed as [35]:

$$\frac{dq_t}{dt} = k_1(q_e - q_t) \tag{10}$$

where q_e and q_t are the amounts of AR18 adsorbed (mg/g) at equilibrium and time t (min), respectively; k_1 is the rate constant of pseudo-first-order kinetic model (1/min). The integrating of Eq. (10) for the boundary conditions $q_t = 0$ at $t = 0$ and $q_t = q_t$ at $t = t$, gives the linear relationship between the amount of AR18 adsorbed (q_t) and time (t).

Table 2
Comparison of maximum adsorption capacity of different adsorbents

Adsorbent	Adsorbate	Conditions	Maximum adsorption capacity (mg/g)	References
SWCNTs	Acid Red 18	–	166.667	Present work
MWCNTs	Methylene Blue	290 K	103.62	[38]
		300 K	109.31	
		310 K	119.71	
F-MWCNTs	Direct Gongo Red	–	148	[2]
	Reactive Green HI-4BD	–	152	
	Golden Yellow	–	141	
MWCNTs- Fe_20_3	Methylene Blue	–	42.3	[39]
	Neutral Red	–	77.5	
CNTs	Procion Red MX-5B	301 K	39.84	[17]
		PH = 6.5		
Halloysite nanotubes	Neutral Red	298 K	54.85	[22]
		308 K	59.24	
Activated carbon	Acid Red 97	–	82.08	[10]
Activated carbon	Methylene Blue	298 K	40.06	[40]
		303 K	40.38	
		318 K	42.86	
Eggshell	Reactive Red 123	–	1.26	[26]

Table 3
Kinetic parameters for the removal of AR18 by SWCNTs at different initial AR18 concentrations

Kinetic model	Dye concentration (mg/L)			
	25	50	75	100
Pseudo-first-order				
q_e, exp (mg/g)	102.786	171.98	205.775	240.27
q_e, cal (mg/g)	4.280	4.544	4.346	4.435
K_1 (1/min)	−0.035	−0.352	−0.035	−0.022
R^2	0.970	0.961	0.941	0.954
Pseudo-second-order				
k_2 (g/mg min)	8.4×10^{-3}	2.38×10^{-3}	9.4×10^{-5}	7.48×10^{-5}
q_e, cal (mg/g)	108.69	181.81	208.33	238.09
R^2	0.994	0.996	0.999	0.999
Intraparticle diffusion				
k_i (mg/(g $min^{1/2}$))	4.470	6.555	5.382	7.023
C_1	51.253	97.321	143.86	157.04
R^2	0.859	0.792	0.745	0.868

$$\ln(q_e - q_t) = \ln(q_e) - k_1 t \quad (11)$$

Values of k_1 can be calculated from the plot of ln ($q_e - q_t$) vs. t for Eq. (11). The values of k_1 and q_e at different initial dye concentration are given in Table 3.

3.6.2. Pseudo-second-order kinetic model

The pseudo-second-order model [36] is based on the assumption of chemisorptions of the adsorbate on the adsorbent. This model is represented as follows:

$$\frac{dq_t}{dt} = k_2(q_e - q_t)^2 \quad (12)$$

Integrating Eq. (12) and noting that $q_t = 0$ at $t = 0$ and $q_t = q_t$ at $t = t$, the following equation is obtained:

$$\frac{t}{q_t} = \frac{1}{k_2 q_e^2} + \frac{1}{q_e} t \quad (13)$$

where k_2 is the equilibrium rate constant of pseudo-second-order (g/mg min). The slope and intercept of the linear plots of t/q_t vs. t gives the values of $1/q_e$ and $1/k_2\ q_e^2$, respectively.

3.6.3. Intraparticle diffusion equation

The kinetic results were analyzed by the intraparticle diffusion model proposed by Weber and Morris to elucidate the diffusion mechanism, since neither the pseudo-first-order nor the second-order model can identify the diffusion mechanism, in which model is expressed as [24]:

$$q_t = k_{id}(t)^{1/2} + C \quad (14)$$

where C (mg/g) is the intercept and k_{id} is the intraparticle diffusion rate constant (mg (g/min)), which is determined from the slope of the linear plots

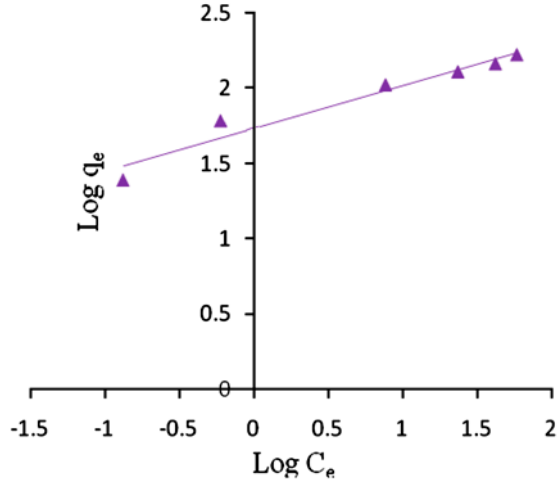

Fig. 7. Freundlich isotherm plot for removal of AR18 by SWCNTs (condition: initial dye concentration = 10, 25, 50, 75, 100, and 120 mg/L, adsorbent dose = .04 g, $T = 25°C$, pH = 7).

of q_t vs. $t^{1/2}$. The values of k_{id} and C along with correlation constant (R^2) for different initial dye concentrations are given in Table 3.

To understand the applicability of the model, linear plots of ln ($q_e - q_t$) vs. t, (t/q_t) vs. t, and q_t vs. $t^{1/2}$ at different dye concentration values for the adsorption of AR18 onto SWCNTs are shown in Fig. 7. Table 3 presented the coefficients of the pseudo-first, pseudo-second-order adsorption kinetic models and the intraparticle diffusion model for different initial dye concentrations. The calculated values of the maximum adsorption capacity (q_e,cal) of the pseudo-first-order kinetic model is far from the experimental values of the maximum adsorption capacity (q_e,exp). Furthermore, in terms of lower correlation coefficient (R^2) values, experimental data did not follow the pseudo-first-order kinetic model. Conversely, the calculated equilibrium adsorption capacity (q_e,cal) of the pseudo-second-order kinetic model is in agreement with experimental data. The correlation coefficients for the pseudo-second-order kinetics model (R^2) are greater than 0.99, confirming the applicability of the pseudo-second-order model and suggest that the adsorption of AR18 onto SWCNTs follows the pseudo-second-order kinetic model. Similar phenomena have been observed for dyes adsorption on CNTs [1,24], halloysite nanotubes [37], and Pine Cone [30] (Figs. 8–11).

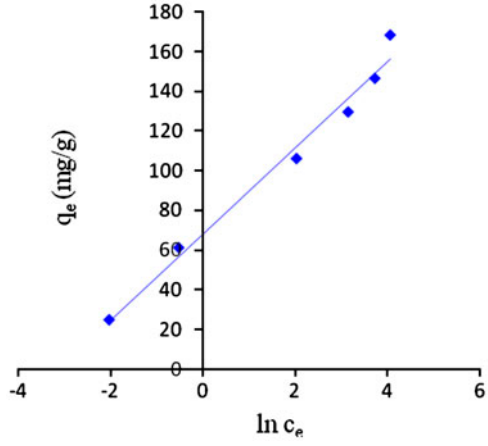

Fig. 8. Temkin isotherm plot for removal of AR18 by SWCNTs (condition: initial dye concentration = 10, 25, 50, 75, 100, and 120 mg/L, adsorbent dose = .04 g, T = 25°C, pH = 7).

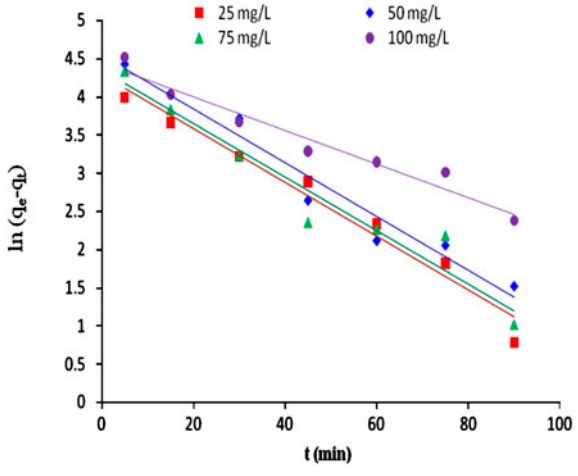

Fig. 9. Pseudo-first-order kinetics plot for removal of AR18 by SWCNTs (condition: initial dye concentration = 25, 50, 75, and 100 mg/L, adsorbent dose = .02 g, T = 25°C, pH = 7).

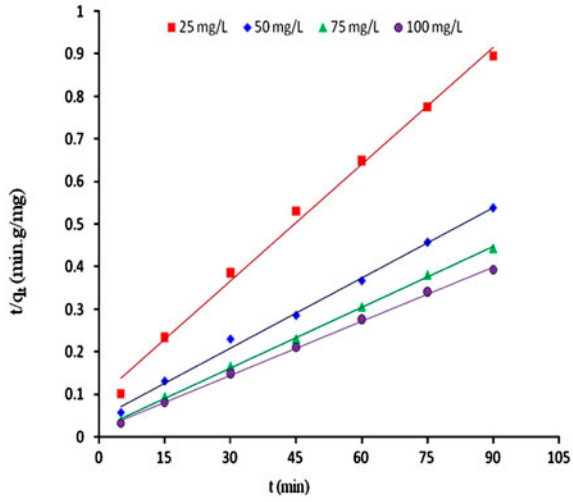

Fig. 10. Pseudo-second-order kinetics plot for removal of AR18 by SWCNTs (condition: initial dye concentration = 25, 50, 75, and 100 mg/L, adsorbent dose = .02 g, T = 25°C, pH = 7).

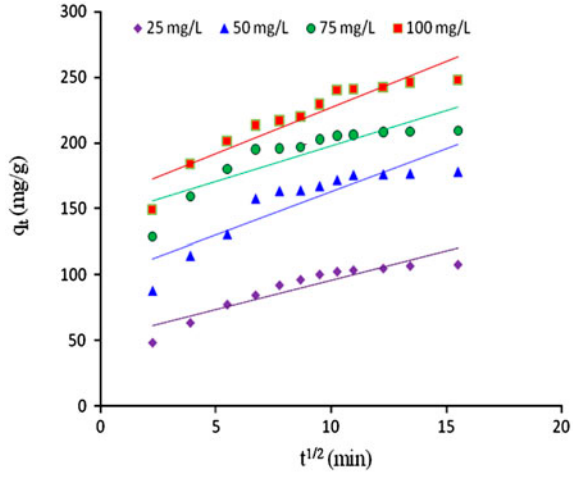

Fig. 11. Intra-particle diffusion plot for removal of AR18 by SWCNTs (condition: initial dye concentration = 25, 50, 75, and 100 mg/L, adsorbent dose = .02 g, T = 25°C, pH = 7).

The results obtained by this research are comparable with the use of MWCNTs [41] and enzymes [42,43] in removal of dyes.

4. Conclusion

Removal of AR18 dye from aqueous solution onto SWCNTs was carried out using a batch technique. Various parameters such as contact time, pH, adsorbent dosage, and initial dye concentration were investigated. The results of this study evidently showed that adsorption equilibriums were reached within 100 min for all initial dye concentration. The maximum dye removal was observed at pH 3.0; an increase in the initial dye concentration decreased the dye removal efficiency, but enhanced the adsorption capacity. The Langmuir, Freundlich, and Temkin isotherms were used to describe how the adsorption molecules distribute between the liquid phase and the solid phase. The results showed that experimental data followed the Langmuir isotherm than the other two isotherms, with maximum adsorption capacity of 166.66 mg/g. The correlation coefficients for the pseudo-second-order kinetics model (R^2) are greater than 0.99, confirming that the adsorption of AR18 onto SWCNTs follows the pseudo-second-order kinetic model.

Acknowledgement

Authors would like to express their gratitude to the Deputy of Research Affair Tehran University of Medical Sciences, for their financial support and assistance.

References

[1] Y. Yao, F. Xu, M. Chen, Z. Xu, Z. Zhu, Adsorption behavior of methylene blue on carbon nanotubes, Bioresour. Technol. 101 (2010) 3040–3046.
[2] A.K. Mishra, T. Arockiadoss, S. Ramaprabhu, Study of removal of azo dye by functionalized multi walled carbon nanotubes, Chem. Eng. J. 162 (2010) 1026–1034.
[3] C.-Y. Kuo, C.-H. Wu, J.-Y. Wu, Adsorption of direct dyes from aqueous solutions by carbon nanotubes: Determination of equilibrium, kinetics and thermodynamics parameters, J. Colloid Interface Sci. 327 (2008) 308–315.
[4] B. Royer, N.F. Cardoso, E.C. Lima, J.C.P. Vaghetti, N.M. Simon, T. Calvete, R.C. Veses, Applications of Brazilian pine-fruit shell in natural and carbonized forms as adsorbents to removal of methylene blue from aqueous solutions: Kinetic and equilibrium study, J. Hazard. Mater. 164 (2009) 1213–1222.
[5] D.S. Brookstein, Factors associated with textile pattern dermatitis caused by contact allergy to dyes, finishes, foams, and preservatives, Dermatol. Clin. 27 (2009) 309–322.
[6] N.K. Amin, Removal of direct blue-106 dye from aqueous solution using new activated carbons developed from pomegranate peel: Adsorption equilibrium and kinetics, J. Hazard. Mater. 165 (2009) 52–62.
[7] M. Iram, C. Guo, Y. Guan, A. Ishfaq, H. Liu, Adsorption and magnetic removal of neutral red dye from aqueous solution using Fe3O4 hollow nanospheres, J. Hazard. Mater. 181 (2010) 1039–1050.
[8] G. Moussavi, M. Mahmoudi, Removal of azo and anthraquinone reactive dyes from industrial wastewaters using MgO nanoparticles, J. Hazard. Mater. 168 (2009) 806–812.
[9] A.H. Mahvi, M. Ghanbarian, S. Nasseri, A. Khairi, Mineralization and discoloration of textile wastewater by TiO_2 nanoparticles, Desalination 239 (2009) 309–316.
[10] V. Gómez, M.S. Larrechi, M.P. Callao, Kinetic and adsorption study of acid dye removal using activated carbon, Chemosphere 69 (2007) 1151–1158.
[11] I.D. Mall, V.C. Srivastava, N.K. Agarwal, I.M. Mishra, Adsorptive removal of malachite green dye from aqueous solution by bagasse fly ash and activated carbon-kinetic study and equilibrium isotherm analyses, Colloid Surface A 264 (2005) 17–28.
[12] A.P. Vieira, S.A.A. Santana, C.W.B. Bezerra, H.A.S. Silva, J.A.P. Chaves, J.C.P. Melo, E.C.S. Filho, C. Airoldi, Removal of textile dyes from aqueous solution by babassu coconut epicarp (*Orbignya speciosa*), Chem. Eng. J. 173 (2011) 334–340.
[13] H. Momenzadeh, A.R. Tehrani-Bagha, A. Khosravi, K. Gharanjig, K. Holmberg, Reactive dye removal from wastewater using a chitosan nanodispersion, Desalination 271 (2011) 225–230.
[14] R.Q. Long, R.T. Yang, Carbon nanotubes as superior sorbent for dioxin removal, J. Am. Chem. Soc. 123 (2001) 2058–2059.
[15] G.-C. Chen, X.-Q. Shan, Y.-Q. Zhou, X.-E. Shen, H.-L. Huang, S.U. Khan, Adsorption kinetics, isotherms and thermodynamics of atrazine on surface oxidized multiwalled carbon nanotubes, J. Hazard. Mater. 169 (2009) 912–918.
[16] J.-L. Gong, B. Wang, G.-M. Zeng, C.-P. Yang, C.-G. Niu, Q.-Y. Niu, W.-J. Zhou, Y. Liang, Removal of cationic dyes from aqueous solution using magnetic multi-wall carbon nanotube nanocomposite as adsorbent, J. Hazard. Mater. 164 (2009) 1517–1522.
[17] C.-H. Wu, Adsorption of reactive dye onto carbon nanotubes: Equilibrium, kinetics and thermodynamics, J. Hazard. Mater. 144 (2007) 93–100.
[18] Y.-H. Li, S. Wang, X. Zhang, J. Wei, C. Xu, Z. Luan, D. Wu, Adsorption of fluoride from water by aligned carbon nanotubes, Mater. Res. Bull. 38 (2003) 469–476.
[19] X. Peng, Z. Luan, Z. Di, Z. Zhang, C. Zhu, Carbon nanotubes-iron oxides magnetic composites as adsorbent for removal of Pb(II) and Cu(II) from water, Carbon 43 (2005) 880–883.
[20] Z.-C. Di, J. Ding, X.-J. Peng, Y.-H. Li, Z.-K. Luan, J. Liang, Chromium adsorption by aligned carbon nanotubes supported ceria nanoparticles, Chemosphere 62 (2006) 861–865.
[21] C. Lu, Y.-L. Chung, K.-F. Chang, Adsorption of trihalomethanes from water with carbon nanotubes, Water Res. 39 (2005) 1183–1189.
[22] P. Luo, Y. Zhao, B. Zhang, J. Liu, Y. Yang, J. Liu, Study on the adsorption of neutral red from aqueous solution onto halloysite nanotubes, Water Res. 44 (2010) 1489–1497.
[23] M. Mohamed, S.K. Ouki, Kinetic and removal mechanisms of ethylbenzene from contaminated solutions by chitin and chitosan, Water Air Soil Poll. 220 (2011) 131–140.
[24] Y. Yao, H. Bing, X. Feifei, C. Xiaofeng, Equilibrium and kinetic studies of methyl orange adsorption on multiwalled carbon nanotubes, Chem. Eng. J. 170 (2011) 82–89.
[25] F.M. Machado, C.P. Bergmann, T.H.M. Fernandes, E.C. Lima, B. Royer, T. Calvete, S.B. Fagan, Adsorption of reactive red M-2BE dye from water solutions by multi-walled carbon nanotubes and activated carbon, J. Hazard. Mater. 192 (2011) 1122–1131.

[26] M.H. Ehrampoush, G. Ghanizadeh, M.T. Ghaneian, Equilibrium and kinetics study of reactive red 123 dye removal from aqueous solution by adsorption on eggshell, Iran. J. Environ. Health Sci. Eng. 8 (2011) 101–108.
[27] E.C. Lima, B. Royer, J.C.P. Vaghetti, N.M. Simon, B.M. da Cunha, F.A. Pavan, E.V. Benvenutti, R. Cataluña-Veses, C. Airoldi, Application of Brazilian pine-fruit shell as a biosorbent to removal of reactive red 194 textile dye from aqueous solution: Kinetics and equilibrium study, J. Hazard. Mater. 155 (2008) 536–550.
[28] S. Senthilkumaar, P. Kalaamani, K. Porkodi, P.R. Varadarajan, C.V. Subburaam, Adsorption of dissolved Reactive red dye from aqueous phase onto activated carbon prepared from agricultural waste, Bioresour. Technol. 97 (2006) 1618–1625.
[29] N.M. Mahmoodi, B. Hayati, M. Arami, Kinetic, equilibrium and thermodynamic studies of ternary system dye removal using a biopolymer, Ind. Crop. Prod. 35 (2012) 295–301.
[30] N.M. Mahmoodi, B. Hayati, M. Arami, C. Lan, Adsorption of textile dyes on pine cone from colored wastewater: Kinetic, equilibrium and thermodynamic studies, Desalination 268 (2011) 117–125.
[31] C.-Y. Kuo, C.-H. Wu, J.-Y. Wu, Adsorption of direct dyes from aqueous solutions by carbon nanotubes: Determination of equilibrium, kinetics and thermodynamics parameters, J. Colloid Interface Sci. 327 (2008) 308–315.
[32] I.A.W. Tan, A.L. Ahmad, B.H. Hameed, Adsorption of basic dye on high-surface-area activated carbon prepared from coconut husk: Equilibrium, kinetic and thermodynamic studies, J. Hazard. Mater. 154 (2008) 337–346.
[33] R. Han, P. Han, Z. Cai, Z. Zhao, M. Tang, Kinetics and isotherms of neutral red adsorption on peanut husk, J. Environ. Sci. 20 (2008) 1035–1041.
[34] S. Hong, C. Wen, J. He, F. Gan, Y.-S. Ho, Adsorption thermodynamics of methylene blue onto bentonite, J. Hazard. Mater. 167 (2009) 630–633.
[35] I.D. Mall, V.C. Srivastava, N.K. Agarwal, I.M. Mishra, Removal of congo red from aqueous solution by bagasse fly ash and activated carbon: Kinetic study and equilibrium isotherm analyses, Chemosphere 61 (2005) 492–501.
[36] Y.S. Ho, C.C. Chiang, Sorption studies of acid dye by mixed sorbents, Adsorption 7 (2001) 139–147.
[37] R. Liu, B. Zhang, D. Mei, H. Zhang, J. Liu, Adsorption of methyl violet from aqueous solution by halloysite nanotubes, Desalination 268 (2011) 111–116.
[38] Z. Shahryari, A.S. Goharrizi, M. Azadi, Experimental study of methylene blue adsorption from aqueous solutions onto carbon nano tubes, Int. J. Water Res. Environ. Eng. 2 (2010) 16–28.
[39] S. Qu, F. Huang, S. Yu, G. Chen, J. Kong, Magnetic removal of dyes from aqueous solution using multi-walled carbon nanotubes filled with Fe_2O_3 particles, J. Hazard. Mater. 160 (2008) 643–647.
[40] Y.C. Sharma, S.N. Upadhyay, F. Gode, Adsorptive removal of a basic dye from water and wastewater by activated carbon, J. appl. sci. environ. sanit. 4 (2009) 21–28.
[41] M. Shirmardi, A. Mesdaghinia, A.H. Mahvi, S. Nasseri, R. Nabizadeh, Kinetics and equilibrium studies on adsorption of acid red 18 (Azo-Dye) using multiwall carbon nanotubes (MWCNTs) from aqueous solution, E. J. Chem. 9 (2012) 2371–2383.
[42] F. Gholami-Borujeni, A.H. Mahvi, S. Nasseri, M.A. Faramarzi, R. Nabizadeh, M. Alimohammadi, Enzymatic treatment and detoxification of acid orange 7 from textile wastewater, J. Appl. Biochem. Biotech. 165 (2011) 1274–1284.
[43] F. Gholami-Borujeni, A.H. Mahvi, S. Naseri, M.A. Faramarzi, R. Nabizadeh, M. Alimohammadi, Application of immobilized horseradish peroxidase for removal and detoxification of azo dye from aqueous solution, Res. J. Chem. Environ. 15 (2011) 217–222.